Available online at www.sciencedirect.com
ScienceDirect
Journal of Power Sources 165 (2007) 379–385
JOURNAL OF POWER SOURCES
www.elsevier.com/locate/jpowsour

Synthesis and characterization of atomic layer deposited titanium nitride thin films on lithium titanate spinel powder as a lithium-ion battery anode

Mark Q. Snyder [a], Svetlana A. Trebukhova [b], Boris Ravdel [b], M. Clayton Wheeler [a], Joseph DiCarlo [b], Carl P. Tripp [c,d], William J. DeSisto [a,c,*]

[a] *Department of Chemical and Biological Engineering, University of Maine, 5737 Jenness Hall, Orono, ME 04469, USA*
[b] *Yardney Technical Products/Lithion Inc., Pawcatuck, CT 06379, USA*
[c] *Laboratory for Surface Science and Technology (LASST), 5708 ESRB-Barrows, Orono, ME 04469, USA*
[d] *Department of Chemistry, University of Maine, Orono, ME 04469, USA*

Received 10 November 2006; received in revised form 7 December 2006; accepted 11 December 2006
Available online 16 December 2006

Abstract

Lithium titanate spinel ($Li_4Ti_5O_{12}$, or LTS) is receiving consideration as a nanopowder anode material for use in lithium-ion batteries. LTS has more positive working potential than traditional graphite anodes, and it does not react with electrolyte components. However, the main drawback of LTS powder is its poor interparticle electronic conductance that reduces the high-rate ability of the electrode. To improve this we have coated the surface of the LTS powder with a titanium nitride layer by atomic layer deposition (ALD). In situ infrared spectroscopy studies were conducted to confirm the attachment of the titanium precursor. The nitrogen content of films was measured by total nitrogen content testing. Transmission electron microscopy (TEM) micrographs confirmed the formation of a thin titanium nitride film around LTS particles by ALD. Finally, lithium cells with electrodes made of original and modified LTS nanopowders were assembled and tested.

Keywords: Lithium titanate spinel; Lithium-ion batteries; Atomic layer deposition; Diffuse reflectance infrared Fourier transform (DRIFT) spectroscopy; Voltage profile; Charge capacity

1. Introduction

Desirable electrode materials for lithium-ion batteries (LIBs) are electronically conductive Li-insertion compounds with a structure that allows lithium mobility. Examples of LIB anodes include lithiated carbon materials and Li alloys. The most commonly distributed LIBs use graphite (or related carbonaceous materials) as anodes. While LIBs substantially reduce power cost, recharging LIBs at high rates remains a challenge. This limitation, to a large extent, is due to lithium metal plating on the surface of the carbon anode at high charging rates. This plating leads to capacity degradation and causes a safety hazard. The origin of lithium metal plating stems from the proximity of the anode potential to that of lithium metal. To avoid lithium plating, the anode charging potential must be less negative.

Lithium titanate spinel (LTS) is an emerging negative electrode material for high rate LIBs [1–18]. Up to three Li ions can be intercalated reversibly per each LTS formula unit, as shown by Eq. (1)

$$Li_4Ti_5O_{12} + 3Li^+ + 3e^- \leftrightarrow Li_7Ti_5O_{12} \quad (1)$$

When fully lithiated, LTS has a specific capacity of 167.5 Ah kg^{-1} and an energy density of 270 Wh kg^{-1} in a Li-metal cell. By comparison, the specific capacity of graphite ranges from 300 to 370 Ah kg^{-1} with an energy density between 380 and 460 Wh kg^{-1}.

Among the advantages of LTS over graphite is its working potential. Since the potential difference between LTS and Li/Li^+ is greater than 1 V, neither a solid electrolyte interphase (SEI)

* Corresponding author at: Department of Chemical and Biological Engineering, 5737 Jenness Hall, Orono, ME 04469, USA. Tel.: +1 207 581 2277; fax: +1 207 581 2323.
E-mail addresses: msnyder@umche.maine.edu (M.Q. Snyder), svetlana@lithion.com (S.A. Trebukhova), bravdel@lithion.com (B. Ravdel), cwheeler@umche.maine.edu (M.C. Wheeler), jdicarlo@lithion.com (J. DiCarlo), ctripp@maine.edu (C.P. Tripp), wdesisto@umche.maine.edu (W.J. DeSisto).

0378-7753/$ – see front matter © 2007 Published by Elsevier B.V.
doi:10.1016/j.jpowsour.2006.12.015

nor a lithium metal will form on the electrode surface regardless of charge rate. Additionally, it may be more stable at elevated temperatures (75–80 °C) because the electrode does not react with the electrolyte components. Without the formation of a SEI, the electrode surface area can be increased through the use of nanoparticulate LTS.

Another advantage of LTS is that it is a "zero-strain" material meaning that lithium ions can be inserted and extracted with minimal change to its lattice dimensions [18]. The ability of a cell to maintain its lattice dimensions is a reliable predictor of its voltage and capacity stability while cycling.

While LTS has many properties that make it a promising alternative to carbonaceous anodes, it has the disadvantage of being a poor electrical conductor (5.8×10^{-8} S cm^{-1} at 140 °C) [19]. Conductive diluents are included in the electrode composite to overcome this problem. Still, more interparticle electrical contact is necessary. We have investigated the modification of the LTS surface chemistry as a means to improve LIB performance. In particular, we have considered coating the particle surface with a layer of TiN.

TiN is a hard, refractory material [20,21] and an excellent metallic-type conductor [20–22]. Atomic layer deposition (ALD) may be an effective means for depositing such a coating. It has been shown that uniform, conformal coatings could be achieved using ALD [20,23,24]. Atomic layer deposition recently has been used to coat the surfaces of powders with SiO_2 [25], TiN [26], and Al_2O_3 [27,28]. The ALD reaction consists of a series of sequential, self-terminating surface half-reactions on a substrate followed by an inert gas purge [20,24,29–31]. In the case of TiN, made from $TiCl_4$ and NH_3, the $TiCl_4$ chemisorbs on to the substrate and, after purging the excess precursor from the system, NH_3 then reacts with the Ti–Cl-terminated surface to form one theoretical monolayer. A detailed description of the reaction chemistry is given in [26]. Actually, only a fraction of a monolayer is formed. Repeated sequential doses of $TiCl_4$ and NH_3 lead to growth of a titanium nitride film on the nanoparticle.

2. Experimental

2.1. ALD materials

The ALD reaction was performed using approximately 0.30 g of lithium titanate spinel powder (Altair Nanomaterials). The as-received nanopowder had a particle diameter of approximately 25 nm, and a measured Brunnauer–Emmett–Teller (N_2) surface area of 69 m^2 g^{-1}. Titanium(IV) chloride (Acros, 99.9%) was used as received. Anhydrous ammonia (Matheson Tri-Gas, 99.99%) was used as the reducing agent and nitrogen source.

2.2. ALD in situ methods

Methods and equipment used to perform the in situ ALD experiments and diffuse reflectance infrared Fourier transform (DRIFT) spectroscopy have been described previously [26]. We used these methods to characterize the surface chemistry of LTS and examine the initial TiN reaction chemistry.

2.3. ALD ex situ methods

2.3.1. Reactor description

The deposition cell was a vertically mounted quartz tube with a porous frit centered axially within the tube to act as a support platform for the powder substrate while allowing the excess precursors to exit the deposition area. A muffle furnace was used to maintain the reaction temperature at 500 °C. The run and vent lines were electrically heated with heating tape to 250 °C to prevent condensation and formation of a $TiCl_4$:NH_3 adduct through weak interactions between the precursors and their adhering to the transfer lines. The pressures upstream and downstream of the reactor were monitored with Baratron differential pressure gauges. The system was equipped with a mechanical vacuum pump and a liquid nitrogen trap. A schematic is provided in Fig. 1.

2.3.2. Precursor delivery

The atomic layer deposition reactor consisted of one stainless steel bubbler to supply the $TiCl_4$. Anhydrous ammonia was supplied by a tank, pressurized to about 2000 Torr. Air-actuated valves regulated precursor delivery via computer software. Titanium(IV) chloride flow was controlled by maintaining bubbler temperature at 0 °C resulting in a vapor pressure of approximately 2.5 Torr. The substrate was exposed to 5×10^6 Langmuirs (10^{-6} Torr-s = 1 Langmuir, L) of $TiCl_4$ followed by a 3-s evacuation and a 2-s nitrogen purge for the first half-cycle. Ammonia flow was controlled by an MKS Instruments Type 247 mass flow controller with a flow rate of 20 standard cm^3 s^{-1} at approximately 2000 Torr. The substrate was exposed to 1.2×10^9 L of NH_3 followed by a 3-s evacuation and a 2-s purge.

2.3.3. Total nitrogen content test

Upon modification of an LTS sample by TiN ALD, 0.15 g of the sample was combusted completely at 1350 °C. The combustion products, NO_x, were measured through the electrical conductivity of the resulting gas.

2.4. Coin cell testing

2.4.1. Coin cell materials

The electrode materials were tested in coin-type cells. The materials were prepared by coating aluminum or nickel foil with slurry consisting of either 80% uncoated or ALD TiN-coated LTS (active material), 10% carbon black (conductive diluent), and 10% polyvinylidene fluoride (PVDF) binder suspended in *N*-methylpyrrolidone. The slurry was manually spread onto the foil with a Gardco Film Applicator (a.k.a. doctor blade) so the thickness of the coating corresponded to a capacity of 0.6–0.8 mAh cm^{-2}.

2.4.2. Coin cell fabrication methods

After coating, the electrodes were calendered, dried under vacuum at 110 °C, and punched to the diameter of 1.3 cm. Lithium foil was used as a counter electrode. A 1 M solution

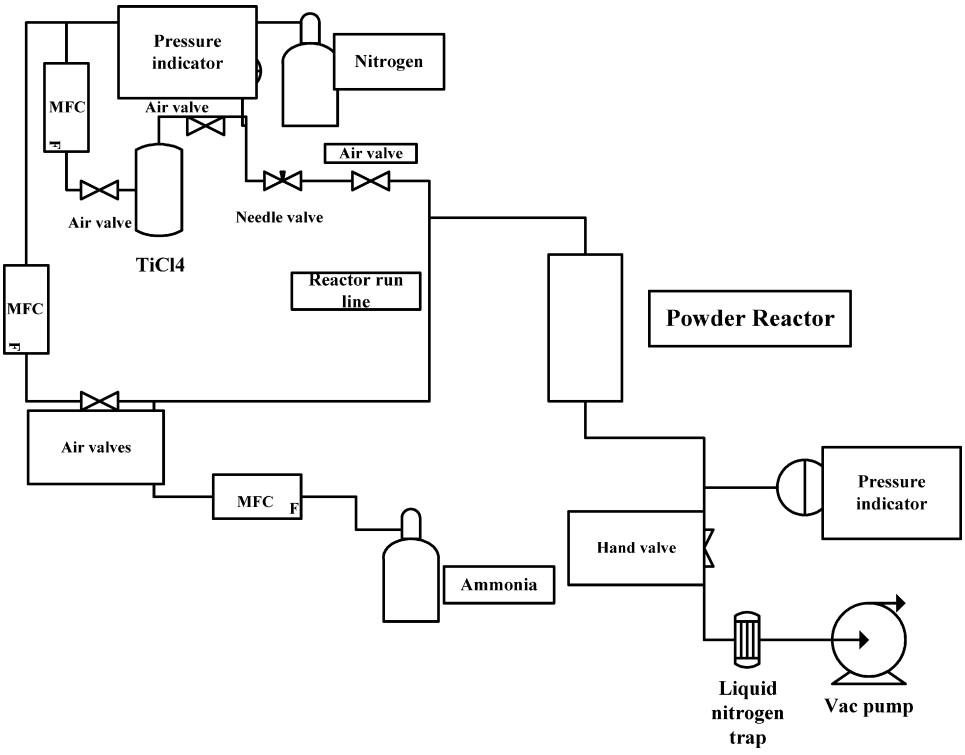

Fig. 1. Schematic of home-built atomic layer deposition reactor.

of $LiPF_6$ dissolved in ethylene carbonate/dimethyl carbonate/diethyl carbonate (Ferro Inc.) mixed 1:1:1 by volume was used as the electrolyte. This electrolyte is typical for lithium-ion cells.

A Setella polyethylene separator, with a thickness of 20 μm, was used.

3. Results

Lithium titanate spinel powder modified by ALD was characterized with in situ and ex situ methods. Analysis with in situ DRIFT spectroscopy was performed to monitor changes to the LTS powder surface after each of the precursors reacted with the substrate and to verify the surface reaction. Modification of the LTS powder also was carried out in a home-built, automated ALD reactor so that a large number of ALD cycles could be deposited.

3.1. ALD with in situ DRIFT characterization

Lithium titanate spinel powder was examined with DRIFT spectroscopy to characterize surface groups and confirm the availability of attachment sites for $TiCl_4$, the first half-reaction in the formation of TiN by ALD. Spectra were collected before and after each surface exposure to $TiCl_4$. The availability of surface hydroxyl groups is a crucial component in functionalizing surfaces and forming thin films. Past work has demonstrated that these hydroxyls are preferred binding sites for metal thin film precursors like $TiCl_4$ [22,30,32,33]. At room temperature, the DRIFT spectrum (Fig. 2a) revealed a small shoulder at 3690 cm^{-1} and a broad peak that stretched from approximately 3410 to 3220 cm^{-1}. These bands were due to isolated metal hydroxyls (M–OH), molecularly adsorbed water, and hydrogen-bonded hydroxyl groups, respectively. A group of absorption bands were observed between 1700 and 1300 cm^{-1}: a peak at 1640 cm^{-1} and a doublet at 1510 and 1460 cm^{-1} with a shoulder at 1350 cm^{-1}. The band at 1640 cm^{-1} represents surface-adsorbed water, while the other peaks were assigned to carbonate impurities, as Li_2O readily absorbs CO_2 [34]. The presence of surface hydroxyls on LTS powder indicated that reaction sites were available for $TiCl_4$.

Fig. 2b is a difference spectrum collected after the addition to the surface and evacuation of $TiCl_4$ vapor. The spectrum of LTS at reaction temperature is used as the reference. Positive bands represent an addition to the surface, while negative bands indicate that a surface group has been removed. Due to the limitations of the environmental chamber, the in situ reaction was performed at 425 °C. The negative band at 3675 cm^{-1} indicates that M–OH groups have shifted downfield because of higher temperatures and have been removed from the surface. Negative bands between 1640 and 1300 cm^{-1} also show that additional carbonate species have been removed as well. The positive band at 940 cm^{-1} represents a Ti–O bond to the surface. Hence, the initial step of reaction of $TiCl_4$ with the LTS was confirmed.

3.2. ALD with ex situ characterization

In addition to the in situ DRIFT studies, TiN was synthesized on LTS powder for further characterization and evaluation as an anode for lithium or lithium-ion cells.

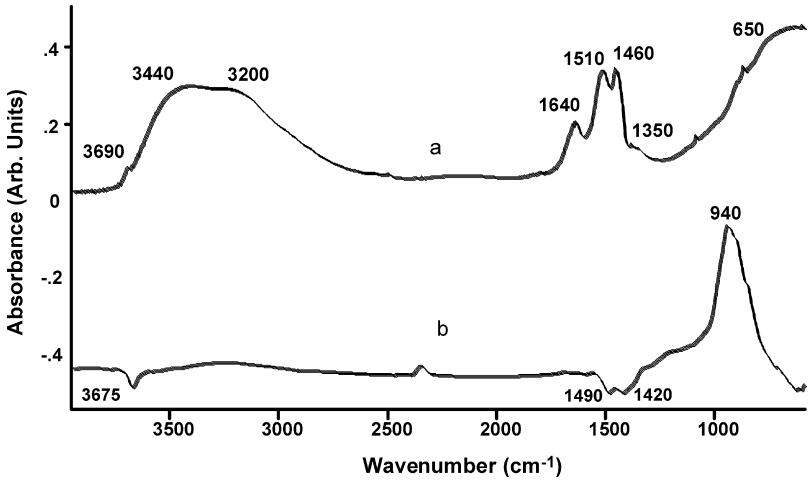

Fig. 2. DRIFT spectrum of LTS at room temperature in air (a) and DRIFT difference spectrum of LTS at 425 °C under vacuum after an addition of $TiCl_4$. The reference is LTS under vacuum at 425 °C (b).

3.2.1. Total nitrogen content

The thickness of the TiN layer is difficult to determine directly because its surface is known to oxidize in air [35–40]. We used the average content of nitrogen in the coated material as the measure of the deposited amount of nitride. A nitrogen content of 0.061% (by weight) was measured for the thin film synthesized by 200 ALD cycles at 500 °C.

3.2.2. TEM analysis

Atomic layer deposition has been shown to coat powders uniformly by other groups [25], and we used transmission electron microscopy (TEM) to verify the uniformity of our coatings. LTS powder, modified with 200 ALD cycles of TiN at 500 °C, was examined with a TEM. Micrographs of unmodified and modified LTS particles are presented in Fig. 3. The unmodified particles (Fig. 3a) appear flat and plate-like. The micrographs of the modified particles show similarly shaped flat, plate-like structures. However, there is a discernible halo of a different density than the rest of the particles (Fig. 3b). While the coating appears uniform, it is difficult to discern whether the specimen shown in Fig. 3b consists of several individual particles or an agglomeration formed by sintering. Determination of the film thickness by visual inspection of the TEM micrographs gives an average thickness of approximately 58 Å, or approximately 0.3 Å $cycle^{-1}$. Assuming the film is stoichiometric TiN, this is slightly greater than the growth per cycle (0.2 Å) for TiN on SiO_2 observed by Ritala et al. [20,41] and similar to the growth per cycle (0.28 Å) for TiN on SiO_2 seen by Satta et al. [42]. The growth per cycle indicates that a non-continuous film is deposited during each cycle.

3.3. Coin cell tests

Figs. 4 and 5 represent the voltage profile and capacity, respectively, of the coin cells during cycling. A cell with LTS modified by TiN ALD was compared to a cell with unmodified LTS. The cells were cycled within 2.2 and 1.4 V at 25 °C. The rate of the first cycle was *C*/20 (*C* is the expected capacity in mAh), followed by two cycles at *C*/10, three at *C*/5, and several more *C*/10 cycles. It is assumed that the product of the LTS reduction, the $Li_7Ti_5O_{12}$, appears as a new phase mechanically mixed with the original species [9]. Since the molar Gibbs energy

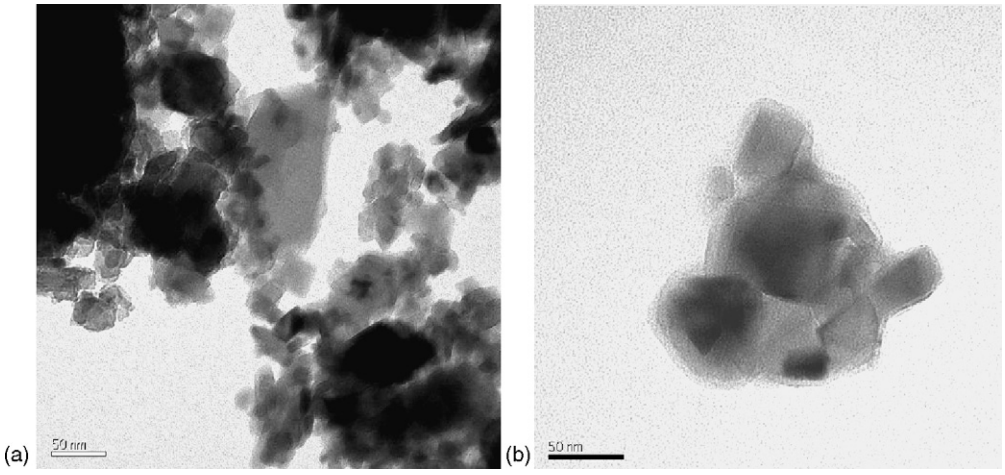

Fig. 3. TEM micrographs of unmodified LTS (a) and LTS modified (b) with 200 cycles of TiN ALD at 500 °C.

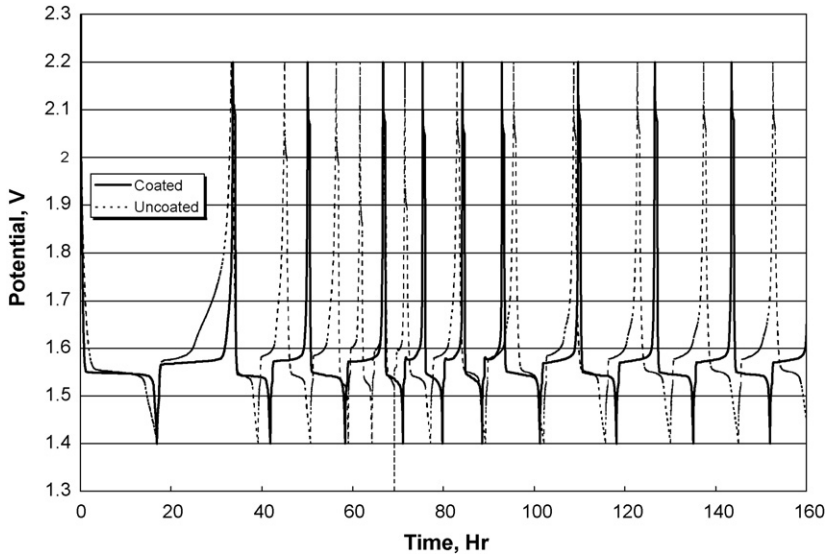

Fig. 4. Cyclic voltammogram of unmodified LTS and LTS modified with 200 cycles of TiN ALD at 500 °C tested as coin-type cells in a lithium-ion battery.

of a two-phase system does not depend on the composition, the voltage of the $Li/Li_4Ti_5O_{12}$ cell should not vary noticeably during lithiation and delithiation at constant current, as has been observed in the literature [9–12].

In Fig. 4, the shape of the voltage–time curve of the cell with unmodified LTS differs from that of the modified LTS. Whereas the discharging branch of the original material reveals a distinctive plateau corresponding to the formation of a two-phase product, the charging branch deviates from the plateau level when the electrode is approximately half-charged. The coulombic efficiency is about 80% of the theoretical maximum during the first cycle, and the electrode capacity decreases significantly during the first several cycles. We assume that the potential increase is due to the crystallite conductance decrease along with delithiation and weakening of the electric contact between the particles. The same effect can be observed in [18]. The slow response of the material is attributed by the authors to poor interparticle electrical contact.

The substitution of the unmodified LTS electrode for LTS coated with TiN via ALD visibly improves the cell performance. Both charging and discharging branches are comprised of relatively long, flat plateaus appearing after a short transient period and followed by abrupt process termination due to a sharp increase (when charging) or decrease (when discharging) of the cell voltage.

The change in specific capacity of the unmodified and modified electrodes brought about by continued cycling and varying charge rates is shown in Fig. 5. The specific charge capacity of the modified electrode nearly maintains its theoretical value over numerous charge/discharge cycles and at different charge rates. Typically, a faster charge rate will decrease charge capac-

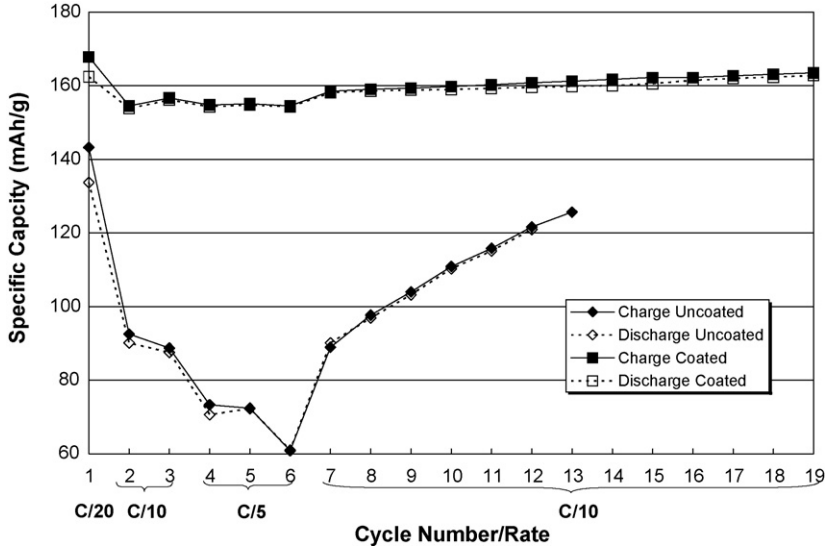

Fig. 5. Measurement of specific capacity of unmodified LTS and LTS modified with 200 cycles of TiN ALD at 500 °C tested as coin-type cells in a lithium-ion battery vs. the number of charge/discharge cycles. The discharge rate is given below the cycle number on the *x*-axis.

ity. However, this is witnessed to only a small extent with the TiN-coated LTS powder coin cell.

The unmodified LTS powder coin cell shows a drastic decrease in specific capacity with increasing charge rate. Ultimately, the cell reaches its lowest specific capacity after the third charge at *C*/5 (sixth overall). Upon decreasing the rate to *C*/10 during the seventh and eighth charge cycles, the specific capacity increases to values similar to those obtained during previous charges at *C*/10. At the ninth and tenth cycles and beyond, an increase in specific capacity occurs. Perhaps this can be attributed to a deformation of the LTS lattice, but otherwise this phenomenon is not readily explained.

4. Discussion

The capacity results indicate the TiN-coated LTS coin cell did not undergo typical capacity fade at higher currents and delivered a constant charge throughout the charging sequence. At higher currents, reduction of the anode occurs only on the outer surface that is coated with an insoluble compound that prevents access to reaction sites in the inner portions of the electrode [43].

It is not clear whether the capacity depends on the rate or if it varies due to macro-structural changes within the electrode upon cycling. Since neither the electrode component composition nor the conductive diluent selection has been optimized, the efficiency improvement in the unmodified electrode particles may be the result of improved interparticle contact while the modified particles have better electrical contact throughout cycling.

Two possible reasons exist for the improved performance of the modified LTS powder over the unmodified powder. The first is the change in particle morphology that occurs at high temperature. Removal of electrically non-conducting carbonate species may also be a contributing factor. The second reason for improved performance was the presence of the TiN thin film. Since the conductance of the LTS is low by nature [11,12], the deposition of a conducting component on its surface may have improved electrical contact. Side reactions with the electrolyte and resistance to fouling by the electrolyte solvent because of the passivating layer may have been averted while preserving the bulk material for Li-ion intercalation.

5. Conclusion

Lithium titanate spinel powder was determined to have surface hydroxyl groups suitable for reaction with $TiCl_4$ to initiate the formation of TiN by ALD. TiN coatings formed by ALD on LTS showed an increase in relative film thickness, as determined by nitrogen content, with an increasing number of deposited layers and with increasing reaction temperature. Manipulation of the NH_3 exposure time indicated that the process is ammonia-starved due most likely to slow surface reaction kinetics.

Coin cell testing indicated that the deposition of a TiN thin film on LTS enhanced LTS electrode performance, possibly through the removal of surface carbonate species and prevention of anode decomposition by the electrolyte. ALD-modified LTS powder produced a constant voltage and sharp process termination upon potential change while either charging or discharging. Cycling tests indicated that the ALD-modified LTS powder maintained a constant charge capacity, close to its theoretical capacity, at various cycling rates. Optimization of the composition of the electrode and the selection of an appropriate binder may enhance performance even further.

Acknowledgements

The authors acknowledge support from Yardney Technical Products Inc. and NSF grant CHE-0346124. The authors also acknowledge Kelly Edwards for performing TEM analysis on the LTS powders.

References

[1] J.L. Allen, J. Wolfenstine, T.R. Jow, 42nd Power Source Conference, Philadelphia, Pennsylvania, 2006, pp. 99–102.
[2] L. Cheng, H.-J. Liu, J.-J. Zhang, H.-M. Xiong, Y.-Y. Xia, J. Electrochem. Soc. 153 (2006) A1472–A1477.
[3] J. Christensen, V. Srinivasan, J. Newman, J. Electrochem. Soc. 153 (2006) A560–A565.
[4] J. Jiang, J. Chen, J.R. Dahn, J. Electrochem. Soc. 151 (2004) A2082–A2087.
[5] A. Du Pasquier, A. Laforgue, P. Simon, J. Power Sources 125 (2004) 95–102.
[6] K. Nakahara, R. Nakajima, T. Matsushima, H. Majima, J. Power Sources 117 (2003) 131–136.
[7] A. Du Pasquier, A. Laforgue, P. Simon, G.G. Amatucci, J.-F. Fauvarque, J. Electrochem. Soc. 149 (2002) A302–A306.
[8] K. Zaghib, M. Simoneau, M. Armand, M. Gauthier, J. Power Sources 81–82 (1999) 300–305.
[9] S. Scharner, W. Weppner, P. Schmid-Beurmann, J. Electrochem. Soc. 146 (1999) 857–861.
[10] D. Peramunage, K.M. Abraham, J. Electrochem. Soc. 145 (1998) 2615–2622.
[11] D. Peramunage, K.M. Abraham, J. Electrochem. Soc. 145 (1998) 2609–2615.
[12] T. Ohzuku, A. Ueda, N. Yamamoto, J. Electrochem. Soc. 142 (1995) 1431–1435.
[13] A. Deschanvres, B. Raveau, Z. Sekkal, Mater. Res. Bull. 6 (1971) 699–704.
[14] N.V. Porotnikov, N.G. Chaban, K.I. Petrov, Izv. Akad. Nauk SSSR, Neorganicheskie Materialy 18 (1982) 1066–1067.
[15] K.M. Colbow, J.R. Dahn, R.R. Haering, J. Power Sources 26 (1989) 397–402.
[16] E. Ferg, R.J. Gummow, A. de Kock, M.M. Thackeray, J. Electrochem. Soc. 141 (1994) L147–L150.
[17] L. Kavan, J. Prochazka, T.M. Spitler, M. Kalbac, M. Zukalova, T. Drezen, M. Gratzel, J. Electrochem. Soc. 150 (2003) A1000–A1007.
[18] L. Kavan, M. Gratzel, Electrochem. Solid-State Lett. 5 (2002) A39–A42.
[19] I.A. Leonidov, O.N. Leonidova, L.A. Perelyaeva, R.F. Samigullina, S.A. Kovyazina, M.V. Patrakeev, Phys. Solid State (Translation of Fizika Tverdogo Tela (Sankt-Peterburg)) 45 (2003) 2183–2188.
[20] M. Ritala, M. Leskelae, E. Rauhala, P. Haussalo, J. Electrochem. Soc. 142 (1995) 2731–2737.
[21] C.J. Carmalt, A.H. Cowley, R.D. Culp, R.A. Jones, Y.M. Sun, B. Fitts, S. Whaley, H.W. Roesky, Inorg. Chem. 36 (1997) 3108–3112.
[22] J.W. Elam, M. Schuisky, J.D. Ferguson, S.M. George, Thin Solid Films 436 (2003) 145–156.
[23] J.-S. Min, Y.-W. Son, W.-G. Kang, S.-S. Chun, S.-W. Kang, Jpn. J. Appl. Phys., Part 1 37 (1998) 4999–5004.
[24] A.W. Ott, J.W. Klaus, J.M. Johnson, S.M. George, Thin Solid Films 292 (1997) 135–144.
[25] J.D. Ferguson, A.W. Weimer, S.M. George, Chem. Mater. 12 (2000) 3472–3480.

[26] M.Q. Snyder, B.A. McCool, J. DiCarlo, C.P. Tripp, W.J. DeSisto, Thin Solid Films 514 (2006) 97–102.
[27] B. Min, J.S. Lee, J.W. Hwang, K.H. Keem, M.I. Kang, K. Cho, M.Y. Sung, S. Kim, M.S. Lee, S.O. Park, J.T. Moon, J. Cryst. Growth 252 (2003) 565–569.
[28] J.R. Wank, S.M. George, A.W. Weimer, J. Am. Ceram. Soc. 87 (2004) 762–765.
[29] M. Juppo, M. Ritala, M. Leskela, J. Electrochem. Soc. 147 (2000) 3377–3381.
[30] S. Haukka, E.L. Lakomaa, A. Root, J. Phys. Chem. 97 (1993) 5085–5094.
[31] E.L. Lakomaa, S. Haukka, T. Suntola, Appl. Surf. Sci. 60–61 (1992) 742–748.
[32] J.P. Blitz, Colloids Surf. 63 (1992) 11–19.
[33] B.J. Ninness, D.W. Bousfield, C.P. Tripp, Colloids Surf., A 214 (2003) 195–204.
[34] H.A. Mosqueda, C. Vazquez, P. Bosch, H. Pfeiffer, Chem. Mater. 18 (2006) 2307–2310.
[35] H.G. Tompkins, J. Appl. Phys. 71 (1992) 980–983.
[36] H.G. Tompkins, J. Appl. Phys. 70 (1991) 3876–3880.
[37] A. Tarniowy, R. Mania, M. Rekas, Thin Solid Films 311 (1997) 93–100.
[38] L.E. Griffiths, A.R. Mount, C.R. Pulham, M.R. Lee, H. Kondoh, T. Ohta, Chem. Commun. (2001) 579–580.
[39] S. Kaskel, K. Schlichte, G. Chaplais, M. Khanna, J. Mater. Chem. 13 (2003) 1496–1499.
[40] F. Esaka, K. Furuya, H. Shimada, M. Imamura, N. Matsubayashi, H. Sato, A. Nishijima, A. Kawana, H. Ichimura, T. Kikuchi, J. Vac. Sci. Technol., A 15 (1997) 2521–2528.
[41] M. Ritala, T. Asikainen, M. Leskela, J. Jokinen, R. Lappalainen, M. Utriainen, L. Niinisto, E. Ristolainen, Appl. Surf. Sci. 120 (1997) 199–212.
[42] A. Satta, J. Schuhmacher, C.M. Whelan, W. Vandervorst, S.H. Brongersma, G.P. Beyer, K. Maex, A. Vantomme, M.M. Viitanen, H.H. Brongersma, W.F.A. Besling, J. Appl. Phys. 92 (2002) 7641–7646.
[43] K. Lahiri, A. Raghunathan, S. Dey, D. Panigrahi, International Conference on VLSI Design/ASP-DAC, Bangalore, India, 2002, pp. 261–267.